Desalination and Water Treatment
www.deswater.com
doi: 10.5004/dwt.2021.27465

230 (2021) 25–32
August

Results of high-efficiency membrane pilot testing for membrane design optimization

F.A. León[a,*], A. Ramos-Martín[b]

[a]*Institute of Intelligent Systems and Numerical Applications in Engineering (SIANI), University of Las Palmas de Gran Canaria, Campus Universitario de Tafira, 35017 Las Palmas de Gran Canaria, Spain, Tel. +0034686169516; email: federico.leon@ulpgc.es*
[b]*Department of Process Engineering, University of Las Palmas de Gran Canaria, Campus Universitario de Tafira, 35017 Las Palmas de Gran Canaria, Spain, email: alejandro.ramos@ulpgc.es*

Received 29 August 2020; Accepted 23 May 2021

ABSTRACT

In a previous paper, we proposed the construction of a new seawater intake in order to reduce the temperature range of the feed water, and a pilot plant for testing three types of low energy and high rejection membranes comparing performance and quality in a seawater reverse osmosis (SWRO) plant in the southeast of Spain. The results of the elements are shown. The conclusions of the study may serve as a tool for the decision-making processes related to membrane replacement and retrofit projects whose designs were based on new high-efficiency membrane configurations in the plant. The selection of the element will be determined regarding the performance and energy costs of the pilot test.

Keywords: Seawater; Reverse osmosis; Desalination; High efficiency; Pilot testing

1. Introduction

In this article, the results are shown of the pilot plant designed in the previous paper [1], testing three reverse osmosis elements from different suppliers in order to select the more convenient one about low energy consumption, high permeate quality, and boron rejection, thanks to the data shared with Acuamed. We have studied the articles of other authors about energy performance in desalination by reverse osmosis [2–13].

The construction of the new seawater intake for the desalination plant in Carboneras (Almería, Spain) was completed immediately before the testing. Since then, the water intake has increased from 14 to 35 m in depth. A new scenario appeared with the lowest maximum temperatures, while the minimum temperatures remained constant as it is shown in Fig. 1. As a result, new designs and opportunities for operational improvements appeared to optimize the process.

The performance of different membranes of three manufacturers is compared to determine the water quality, under a more stable thermal scenario, from the analysis of the electrical conductivity, temperature, and others. After the aging phase for 7 months, the pilot test is running 15 d per element to get more realistic results of feed pressure, permeate conductivity, and boron. These data were needed for choosing the most appropriate element for this SWRO plant.

Following the state of the art in water desalination and the evolution of this process for a national and international level, there are different desalination processes such as vapor compression (VC), multi-effect distillation (MSF), multi-stage distillation (MED), and reverse osmosis, which currently accounts for 65% of the total in the world [1–2].

This paper also studies the improvements in seawater desalination, based on the reduction of energy consumption in the production of freshwater. Consequently, reverse osmosis is the most suitable process due to its lower energy consumption per cubic meter of water produced, and therefore, it occupies a privileged position in the sector. So far, in the 21st century, research efforts in water desalination have focused on advances in reverse osmosis membranes, with higher surface area and lower

* Corresponding author.

energy consumption, as well as energy recovery systems to recover the brine pressure and to introduce it in the system reducing the energy consumption of the desalination process. The operation, maintenance, and handling of the membranes have been studied in detail, due to their importance in energy savings, showing how to optimize all the processes in which they are involved to improve energy efficiency [3–5].

Energy efficiency in desalination plants depends on the quality of permeate water required, in this case in Spain according to the Royal Decree 140/2003 of February 7th, following the sanitary criteria of the quality of the water of human consumption established. Boron is the highest restriction issue of all the ions, and it must be lower than 1 ppm. Therefore, sometimes it requires a second pass of the permeate water or high rejection membranes operating with higher pressures, that is, consuming more energy and increasing this cost which is also one of the most significant of the variable costs of the installation [6–9].

2. Pilot test description

As described in the previous article [1], the elements tested from three different suppliers (A, B, and C), are as given in Table 1.

Regarding the test conditions of the tested elements, the feed water pressure is 800 psi (5.52 MPa), feed water concentration 32,000 mg/L NaCl, feed water temperature 77°F (25°C), feedwater pH 8, and recovery rate 8%.

The pressure vessel of the pilot test is equipped with flow meters for the permeate and brine, control valves for the feed and brine, and pressure transmitters for the feed and brine as specified in the previous article [1].

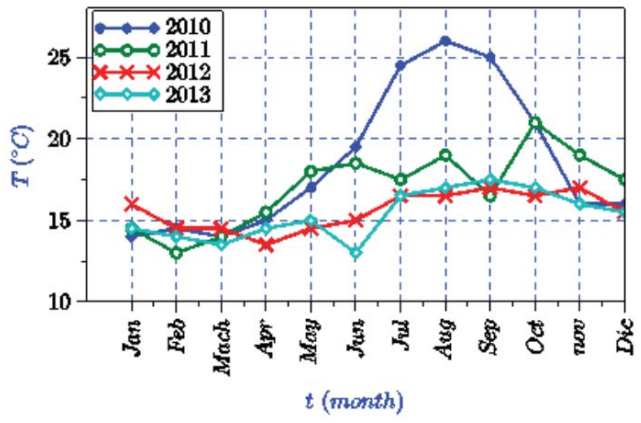

Fig. 1. Monthly raw seawater temperatures.

In summary, there is one pilot vessel and three aging vessels in parallel with all the vessels of train 1 of Carboneras SWRO Plant, which has 12 trains of 10,000 m^3/d each one with the high-pressure vessel, electric motor, and Pelton turbine. The pilot vessel has a capacity of 3.6 m^3/h with seven elements in series. The pilot test developed consists of three aging high-pressure vessels (HPV) and a Test HPV.

2.1. Aging HPV description

Aging HPV consists of three high-pressure vessels. The vessels are equipped with a control valve, a pressure transmitter, and a flow meter in the permeate flow. Further instruments of the rack provided the necessary information for the appropriate Aging HPV monitoring. The aim of the aging HPV was to achieve a mature performance of the membranes, Fig. 2 displays the diagram of the aging HPV. During this aging process, 2 months, the main performance parameters have been controlled.

The three pressure vessels (Aging HPV) are installed in parallel with the other vessels of the train. It is introduced the same feed flow and same feed pressure for all three pressure vessels.

2.2. Test HPV description

Test HPV consists of a vessel equipped with all the required elements in order to fully monitoring and control the operational conditions (pressure and flows of the seawater, brine, and permeate flows).

The Test HPV was equipped with:

- Feed seawater flow:
  - a control valve at the HPV inlet for the water flow and pressure control,
  - a pressure transmitter,
  - a drop pressure transmitter,
- Permeate flow:
  - a flow meter,
  - a pressure transmitter (the one of the full-scale rack),
- Brine flow:
  - three valves, in order to control the brine flow and appropriately make the brine discharge from 65 bars to atmospheric pressure.
  - a flowmeter.

Table 1
Details of the membranes. Membrane area 440 ft^2 (41 m^2), feed spacer thickness 28 mm, diameter 8 inch

Model	Number of elements	Average flow (m^3/d)	Average boron rejection at pH 8 (%)	Average TDS rejection (%)
A R-440	7	33.2	95	99.85
B 440-R	7	36.9	93	99.78
C R-440	4	24.8	89	99.85
C X-440	3	35.4	93	99.63

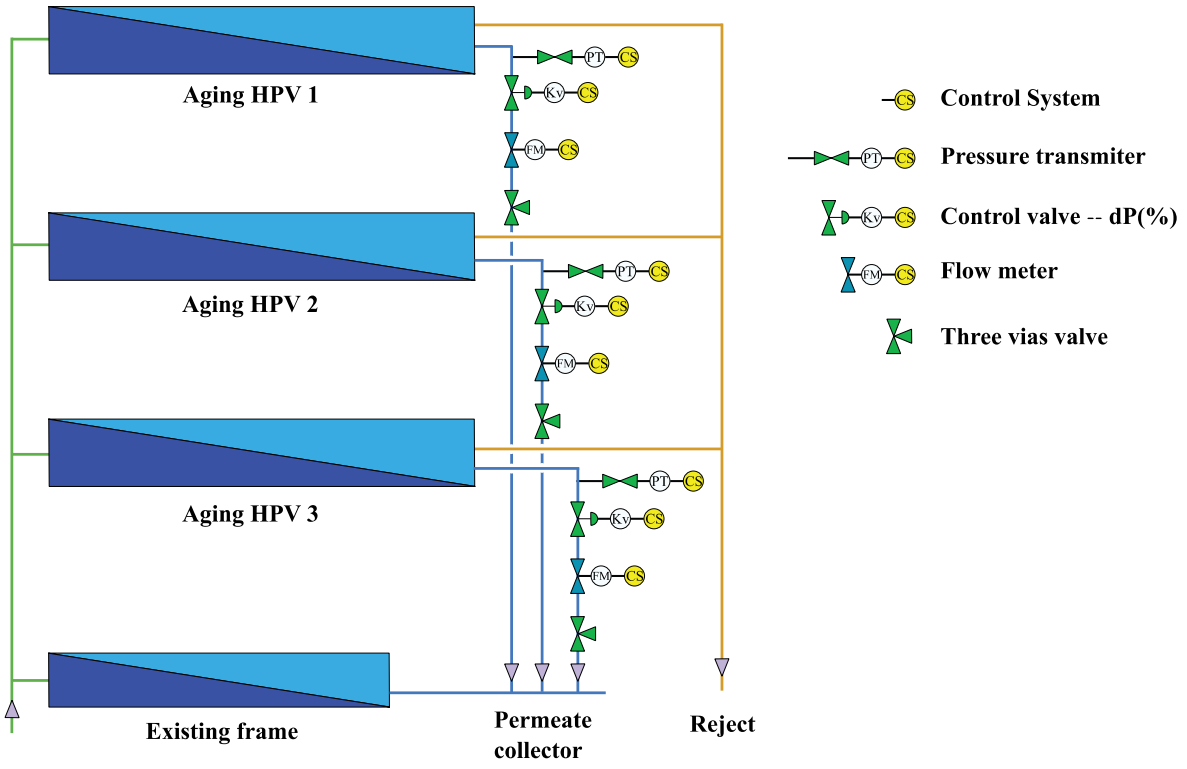

Fig. 2. Aging HPV diagram.

For the test HPV, the feed flow was calculated by summing up brine and permeate flows.

The test HPV was designed to make it possible to test the three membrane types, each one from each manufacturer, under any condition. Test HPV diagram is shown in Fig. 3. Any operation parameter (pressure or flow) could be modified by the control valves, and every main parameter (pressure, flows, and water quality) could be measured.

The membranes tested, to determine its performance, have been subjected to the same operating conditions (pressure, flow, and temperature).

Also, it has been installed at the permeate pipe: a flow meter, a pressure transmitter, and a three vie valve. Moreover, it has been installed instruments in the brine pipe (three valves and a flow meter) and in the feed pipe (pressure transmitter, drop pressure transmitter, and a control valve for the pressure and water flow control).

Under these conditions, it is possible to test the three different models of reverse osmosis membranes under real conditions, changing the feed pressure or feed flow, in order to get a permeate flow and also variating the recovery of the system. After this pilot test and with the information of the aging vessels, it can be obtained different schemas of the efficiency of each membrane, to select the most efficient element.

3. Sequential methodology of the pilot test

The testing has been operating for 15 d for each element, after the aging phase of 2 months running simultaneously, under the same conditions.

In the case of the pilot testing, the elements have been operating separately and the obtained results have been compared under the same conditions of pressure, temperature, and flow.

The important issue was to design the hydraulic system according to the operational conditions, the definition of the parameters and main criteria for the testing, the piping system, and the control valves of the pilot test.

4. Energy consumption and carbon footprint

Energy consumption is mathematically represented by the expression of the following equation in an approximate way:

$$h_{b(\text{año } 1-5)} = (a\, t_m + b) + h_{b(\text{año } 0)} \quad (1)$$

Constants "a" and "b" depending on the temperature, the feed quality, type of intake, and recovery.

In the same way, the real power of the pump is calculated by dividing the theoretical power by its efficiency and the energy in kWh working 24 h a day [10–15].

$$P_{\text{real}b} = P_b/\eta \quad (2)$$

$$P_b = \rho\, g\, Q\, h_b \quad (3)$$

where t_m is the age of the membrane; $P_{\text{real}b}$ is the real power of the pump; P_b is the theoretical power of the pump (in Watts; 1 Hp = 745.7 W); ρ is the density of the fluid (1,000 kg/m^3 in the case of water); g is the acceleration of

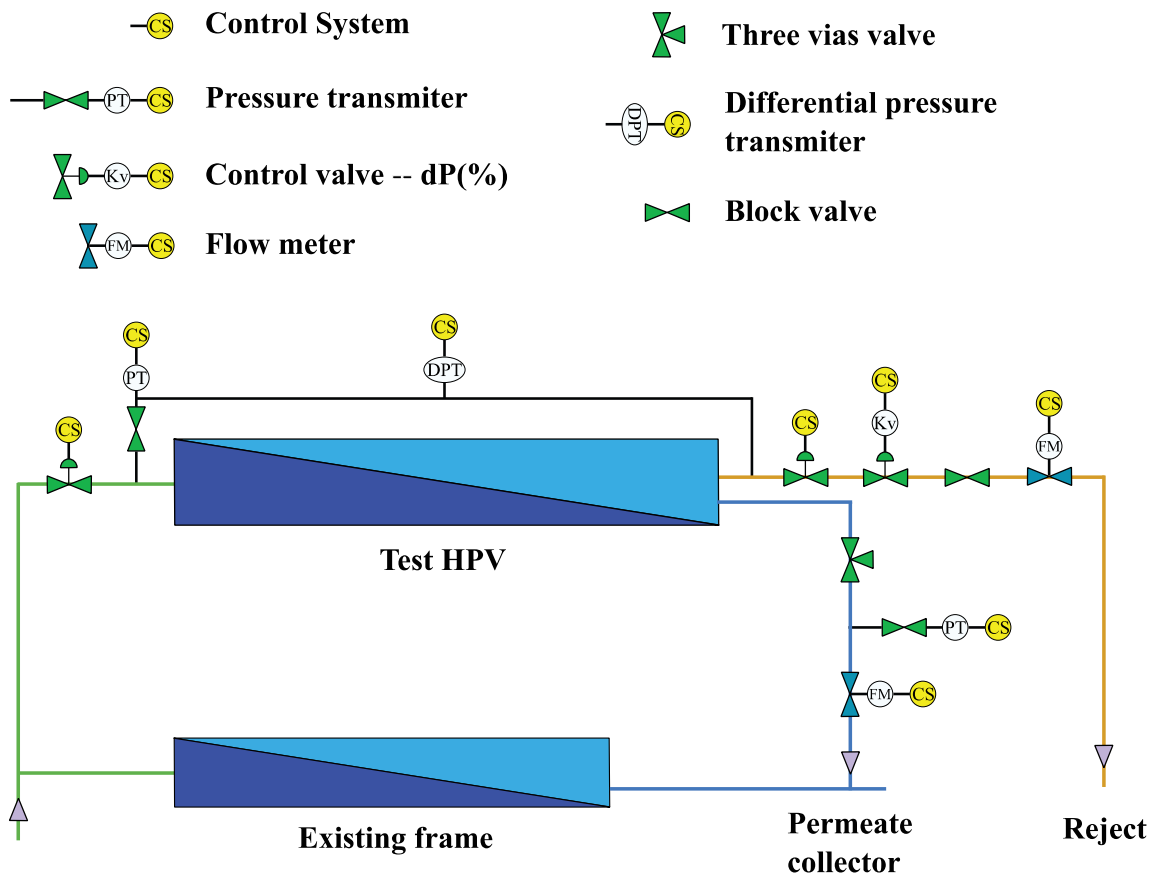

Fig. 3. Test HPV diagram.

gravity (generally adopted: 9.81 m/s^2); η is the performance of the pump; Q is the flow rate (m^3/s); h_b is the pump head (m).

Energy consumption could be also calculated using the Toray DS software from Toray Industries, Inc. (RO membrane manufacturer).

Moreover, it is calculated the carbon footprint of the current and future energy mix, considering the sum of the energies of each technology and its emissions mix factor.

$$HC_{MIX} = \Sigma E_i FM_i \quad (4)$$

where HC_{MIX} is the carbon footprint of the energetic mix (tCO_2); E_i is the energy of each technology (kWh); FM_i is the emission factor of the electric mix (tCO_2/kWh).

5. Results and discussion

Fig. 4 shows the required feed pressure to produce the set permeate flow value at different feedwater temperatures. During all this testing feed seawater pH has been 8.0, with no fluctuations while the pilot has been operating.

Results show pressure requirements to get the set to permeate flow value. Since pressure is related to pump energy consumption, from this Fig. 4, the energy efficiency of the membranes may be inferred. Average feed pressure values at the 20°C range are shown in Table 2.

Feed pressure requirements resulted in different estimated power requirements [6]. Pressure and power requirements approach a linear relation. Thus, pressure requirements (and power requirements) for B-membranes membranes were 2% above A-membranes, and C-membranes were 3% above A-membranes.

Fig. 5 shows permeate conductivity at different feed temperature values for the different membranes.

Conductivity during the testing stage was lower than conductivity during the aging stage for the same temperature, as to permeate set flow at the testing stage was higher [5] (Table 3).

Fig. 6 shows permeate boron concentration at different temperatures. It is important to point out that there are only three available values of boron concentration for A-membranes because of an analytical problem detected at the initial boron determinations. Hence, such values were dismissed.

Table 4 shows the average boron values at 17°C–19°C range.

The pilot test with the three types of membranes has been operated to study the energy consumption after the test, that is, after 151 d of aging plus 2 months of a pilot test for a total of 211 d of operation, that is, 0.58 y. In addition, it is estimated the results that we would obtain after 5 y of operation with these types of membranes without replacement and with 10%, 15%, and 20% annual

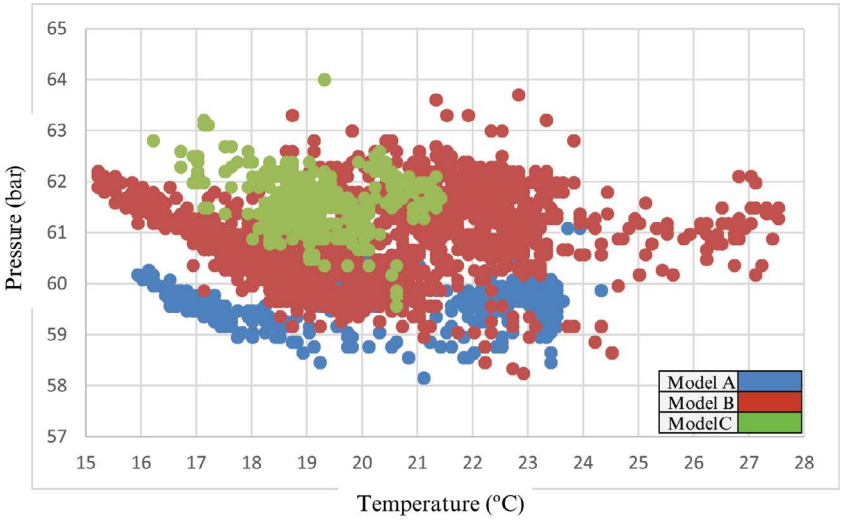

Fig. 4. Feed pressure evolution with temperature during the testing stage.

Table 2
Feed pressure (bar) at 19°C–21°C range

Feed pressure (bar)	Membranes		
	A	B	C
Average	59.6	60.7	61.4
Standard deviation	0.64	0.87	0.52
Population	280	372	193
Average temperature (°C)	19.9	20.0	19.7

cumulative replacement; considering the Pelton turbine currently available, and the potential option of introducing ERI energy recuperators in the best energy-saving scenario at 20% annual replacement for 5 y. For this purpose, the pressure and the energy consumption are shown and compared in Tables 6–8.

These results have been considered with Pelton turbine and ERI energy recovery, with the different low-energy membranes of the three manufacturers, for a permeate flow of 3.6 m^3/h, 44.3% recovery, and approximately 211 operating days (0.58 y) at average temperature according to Table 5.

Regarding item 4 and Eqs. (1)–(4), based on pilot test conditions of Table 5, it is calculated energy consumption in Tables 6–8 and carbon footprint of this pilot test in Table 9, using the average values of energy consumption between the year 0 and 5 with and without replacement. It is considered the emission factor of electric mix in the Spanish mainland FM_i = 0.2628 tCO_2/kWh from Red Eléctrica Española, S.A.

Calculations with a 10% replacement per year during 5 y of operation assume an average age of the membranes of 3.50 y, considering a 15% replacement it is 2.75 y, and for 20% the estimated average age is 2.00 y. In this sense, it

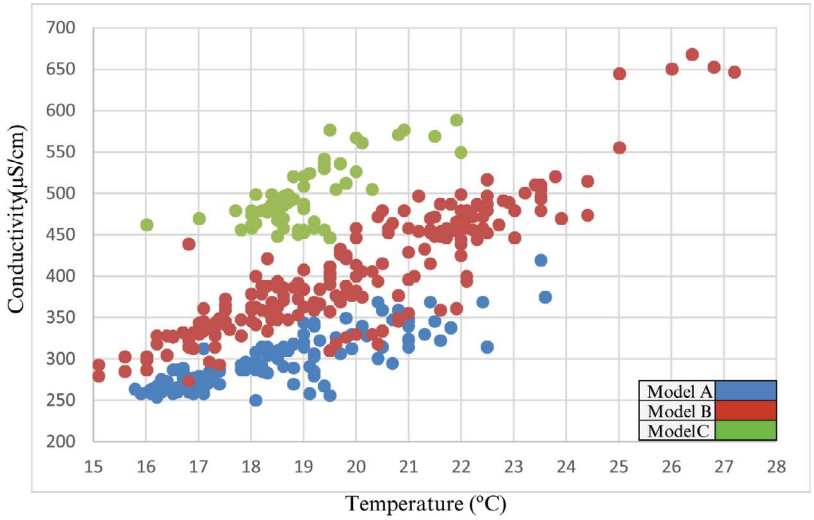

Fig. 5. Conductivity evolution with temperature during the testing stage.

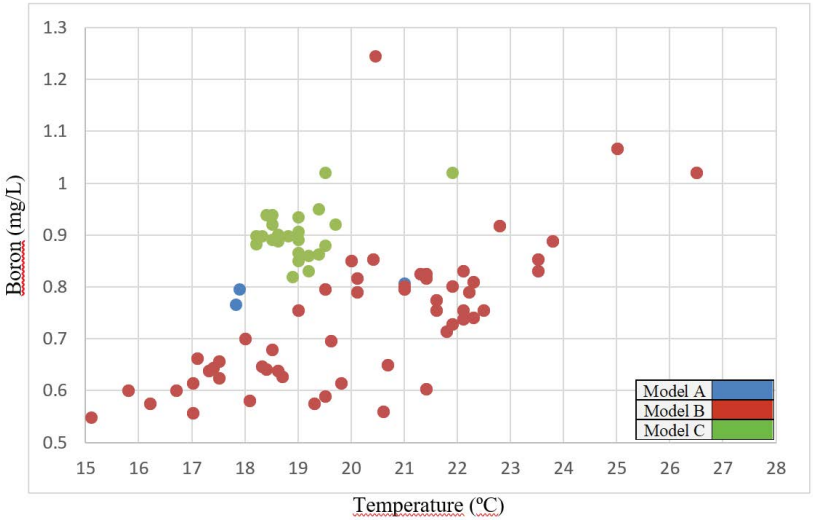

Fig. 6. Permeate boron concentration evolution with temperature during the testing stage.

Table 3
Average permeate conductivity at 19°C–21°C range

Conductivity (µS/cm)	Membranes		
	A	B	C
Average	319.3	394.6	522.9
Standard deviation	32.49	45.4	42.4
Population	26	45	18
Average temperature (°C)	19.8	20.0	19.7

Results show that the lower conductivity belonged to A-membranes, followed by B-membranes (24% higher), and C-membranes (64% above B-membranes).

Table 4
Average permeate boron concentration at 17°C–19°C range

Boron (mg/L)	Membranes		
	A	B	C
Average	0.8	0.6	0.9
Standard deviation	0.02	0.04	0.03
Population	2	6	11
Average temperature (°C)	17.7	17.8	18.5

Results show that B-membranes reject boron better than A-membranes (with boron permeate concentration 21% above B-membranes) and C-membranes (with boron permeate concentration 39% above B-membranes)

is shown how the type A-membrane is more efficient than the rest, to carry out replacements, and even if it is possible in the future to introduce an energy recovery system. In the scenario without replacement and 5 y of operation with membrane C, the energy consumption is the worst case about 3.585 kWh/m^3 considering the Pelton turbine. On the other hand, in the most favorable scenario with membrane A and 20% replacement including ERI, the energy consumption is only 2.346 kWh/m^3.

Table 5
Pilot test conditions

Average flux (lmh)	12.6
Temperature (°C)	20
Recovery (%)	44.3
Feed salinity (g/L)	39.9
Permeate flow (m^3/h)	3.6

Table 6
Pressure, power, and energy consumption of the membrane A

Year	Pressure (bar)	Power (kW)	Pelton/ERI (kW)	Energy (kWh/m^3)
0.58	59.60	17.31	5.17	3.372
5 (0%*R*)	61.56	17.88	5.34	3.483
5 (10%*R*)	60.98	17.71	5.29	3.450
5 (15%*R*)	60.67	17.62	5.26	3.432
5 (20%*R*)	60.34	17.52	5.23	3.414
5 (20%ERI)	61.63	8.45	7.56	2.346

Moreover, about energy consumption in kWh/m^3 of water produced, it could be also calculated using the Eqs. (1)–(3) based on the different energy recovery systems available in seawater desalination plants. Therefore, they are shown the following examples being the power:

- 2.61 kWh/m^3 if there are isobaric chambers (ERI, DWEER, etc.)
- 3.04 kWh/m^3 if a Pelton turbine or similar is available, and
- 3.50 kWh/m^3 with Francis or other turbine type systems

Following Eqs. (1)–(4), the carbon footprint is calculated. This is done for the case of the lowest energy consumption with membrane A and for the scenario of highest energy consumption with membrane C, using

the average values of energy consumption between years 0 and 5 with and without replacement, as shown in Table 9. For all this, we have considered the Peninsula mix factor governed by Red Eléctrica Española, S.A.

6. Conclusions

The construction of the new seawater catchment at the Carboneras desalination plant (from 14 to 35 m depth) changed the thermal scenario. While the minimum temperatures stayed the same, maximum temperatures were lower. Hence, new opportunities for the membrane-system design appeared. Thus, a pilot test was developed in order to test the optimal membrane configuration able to fulfill quality and quantity needs with minimum energy consumption.

The pilot test was defined into two phases: the aging and the testing stage. The aging stage is aimed at achieving a mature performance of the membranes. The testing stage allowed better control of the operational parameters, therefore, obtaining quality data to be analyzed.

Results show a certain dispersion of data (especially related to those of feed pressure and correlation among normalized data) that may be corrected with the improvement of control elements (valves). An increase of boron results related to A-membranes membranes would be more appropriate, and it would be suitable to test C-membranes membranes at higher temperatures. Therefore, new resources would be required to continue the experiments. Nevertheless, the results achieved the objectives of the study to compare the performance and to determine the optimal membrane configuration.

According to the results, A-membranes were the most efficient membranes (with 59.6 bar required to produce 4.05 m^3/h in a seven-element HPV at 20°C range), followed by B-membranes membranes (with pressure requirements 2% higher) and C-membranes membranes with pressure requirements of 3% above A-membranes).

Concerning permeate quality, A-membranes offered the lowest salinity (152 μS/cm normalized conductivity), followed by B-membranes (37% more salinity) and C-membranes (74% above A-membranes). In contrast to this, B-membranes produced permeate with a lower boron concentration (0.8 mg/L at 18°C range), followed by A-membranes (21% above B-membranes) and C-membranes (39% above B-membranes).

Table 10 hierarchically organized the performance of the membranes.

According to the results and classification, the best option would depend on water quality requirements (boron/salinity) and energy efficiency needs for the desalinated water production.

Table 7
Pressure, power, and energy consumption of the membrane B

Year	Pressure (bar)	Power (kW)	Pelton/ERI (kW)	Energy (kWh/m^3)
0.58	60.70	17.63	5.27	3.434
5 (0%*R*)	62.66	18.20	5.44	3.544
5 (10%*R*)	62.07	18.03	5.39	3.511
5 (15%*R*)	61.76	17.94	5.36	3.494
5 (20%*R*)	61.44	17.84	5.33	3.476
5 (20%ERI)	62.73	8.59	7.70	2.386

Table 8
Pressure, power, and energy consumption of the membrane C

Year	Pressure (bar)	Power (kW)	Pelton/ERI (kW)	Energy (kWh/m^3)
0.58	61.40	17.83	5.32	3.473
5 (0%*R*)	63.40	18.40	5.50	3.585
5 (10%*R*)	62.80	18.23	5.45	3.552
5 (15%*R*)	62.49	18.14	5.42	3.534
5 (20%*R*)	62.16	18.04	5.39	3.515
5 (20%ERI)	63.45	8.68	7.78	2.412

Table 9
Carbon footprint for the cases with highest and lowest energy consumption

Carbon footprint (HC) $kgCO_2/m^3$		
Technology	Membrane A	Membrane C
HC 5 y 0%	0.9083	4.4506
HC 5 y 10%	0.9039	4.4292
HC 5 y 15%	0.9015	4.4175
HC 5 y 20%	0.8991	4.4058
HC 5 y 20% ERI	0.7576	3.7124

Table 10
Summary of the results

	Membranes		
	A	B	C
Feed pressure (bar)	59.6	60.7	61.4
Conductivity (μS/cm)	319.3	394.6	522.9
Boron (ppm)	0.8	0.6	0.9

Acknowledgments

This research has been co-funded by the INTERREG V-A Cooperation, Spain-Portugal MAC (Madeira-Azores-Canarias) 2014–2020 program, and MITIMAC project (MAC2/1.1a/263).

References

[1] F.A. Leon, A. Ramos, Analysis of high efficiency membrane pilot testing for membrane design optimization, Desal. Water Treat., 73 (2017) 208–214.
[2] E. Dimitriou, E. Mohamed, Experimental comparison of the performance of two reverse osmosis desalination units equipped with different energy recovery devices, Desal. Water Treat., 55 (2015) 3019–3026.
[3] E. Dimitriou, E. Mohamed, G. Kyriakarakos, G. Papadakis, Experimental investigation of the performance of a reverse

osmosis desalination unit under full-and part-load operation, Desal. Water Treat., 53 (2015) 3170–3178.
[4] F.J.G. Latorre, S.O.P. Báez, A.G. Gotor, Energy performance of a reverse osmosis desalination plant operating with variable pressure and flow, Desalination, 366 (2015) 146–153.
[5] J. Kherjl, A. Mnif, I. Bejaoui, B. Hamrouni, Study of the influence of operating parameters on boron removal by a reverse osmosis membrane, Desal. Water Treat., 56 (2015) 2653–2662.
[6] J.S. Rodriguez, J.M. Veza, A.B. Marigorta, Energy efficiency and desalination in the Canary Islands, Renewable Sustainable Energy Rev., 40 (2014) 741–748.
[7] N. Dow, S. Gray, J. Li, J. Zhang, E. Ostarcevic, A. Liubinas, P. Atherton, G. Roeszler, A. Gibbs, M. Duke, Pilot trial of membrane distillation driven by low grade waste heat: membrane fouling and energy assessment, Desalination, 391 (2016) 30–42.
[8] N.M. Mazlan, D. Peshev, A.G. Livingston, Energy consumption for desalination – a comparison of forward osmosis with reverse osmosis, and the potential for perfect membranes, Desalination, 377 (2016) 138–151.
[9] N.R.G. Walton, Electrical conductivity and total dissolved solids – what is their precise relationship?, Desalination, 72 (1989) 275–292.
[10] S. Boerlage, N. Nada, Algal toxin removal in seawater desalination processes, Desal. Water Treat., 55 (2015) 2575–2593.
[11] T. Bilstand, E. Protasova, A. Simonova, S. Stornes, I. Yuneizi, Wind-powered RO desalination, Desal. Water Treat., 55 (2015) 3106–3110.
[12] V.G. Gude, Desalination and sustainability – an appraisal and current perspective, Water Res., 89 (2016) 87–106.
[13] D. Song, Y. Wang, S. Xu, J. Gao, Y. Ren, S. Wang, Analysis, experiment and application of a power-saving actuator applied in the piston type energy recovery device, Desalination, 361 (2015) 65–71.
[14] J. Kitzes, A. Galli, M. Bagliani, J. Barret, G. Dige, S. Ede, K. Erb, S. Giljum, H. Haberl, C. Hails, L.J. Ferrier, S. Jungwirth, M. Lenzen, K. Lewis, J. Loh, N. Marchettini, H. Messinger, K. Milne, R. Moles, C. Monfreda, D. Moran, K. Nakano, A. Pyhala, W. Rees, C. Simmons, M. Wackernagel, Y. Wada, C. Walsh, T. Wiedmann, A research agenda for improving national Ecological Footprint accounts, Ecol. Econ., 68 (2009) 1991–2007.
[15] M. Lenzen, S.A. Murray, B. Korte, C.J. Dey, Environmental impact assessment including indirect effects - a case study using input–output analysis, Environ. Impact Assess. Rev., 23 (2003) 263–282.